24th COBEM - 2017

24th ABCM International Congress of Mechanical Engineering
December 3-8, 2017, Curitiba, PR, Brazil

COBEM-2017-2687
FIRST RESULTS OF THE CAVITATION EROSION BEHAVIOR FOR LOW-TEMPERATURE PLASMA CARBURIZED MARTENSITIC STAINLESS STEEL

Fabiane da Silva Severo
Rodrigo Perito Cardoso
Silvio Francisco Brunatto
Plasma Assisted Manufacturing Technology and Powder Metallurgy Group, Universidade Federal do Paraná, Curitiba-PR, 81531-980, Brazil
severo.fabiane@gmail.com
rodrigo.perito@ufpr.br
brunatto@ufpr.br

Cristiano José Scheuer
Plasma Assisted Manufacturing Technology and Powder Metallurgy Group, Universidade Federal do Paraná, Curitiba-PR, 81531-980, Brazil
Industrial Technical College, Universidade Federal de Santa Maria, Santa Maria-RS, 97105-900, Brazil
cristiano.scheuer@gmail.com

Abstract. *This work presents first results of the investigation regarding the cavitation erosion resistance of a plasma carburized martensitic stainless steel (MSS). AISI 420 MSS was DC plasma carburized at 350 °C for 12 h using a gas mixture of 99.5% (80% H_2 + 20% Ar) + 0.5% CH_4. Samples were characterized by X-ray diffractometry and microhardness measurements. Cavitation erosion tests were performed on treated (carburized) and untreated (quenched and 220 °C tempered) samples, according to the ASTM G32-10 standard (ultrasonic vibratory apparatus). The characteristics of the damaged surfaces were analyzed by means of scanning electron microscopy, in order to identify the main wear mechanisms. XRD results evidence the formation of a layer composed by carbon-expanded martensite (α'_C) and cementite (Fe_3C) phases, which exhibits hardness about 1.3 times higher to the untreated material. These first results of cavitation tests demonstrated that the superficial increase on carbon content, using the plasma technique, leads to the improvement on the cavitation erosion resistance of the treated material, since it promotes the hard carburized layer formation that enhances the material's capacity in responding to cavitation. Nominal incubation periods of 7.8, and 17.9 h for the untreated, and carburized samples were observed, respectively.*

Keywords: *Cavitation erosion, AISI 420 martensitic stainless steel, low temperature plasma carburizing, carbon-expanded martensite*

1. INTRODUCTION

Local pressure fluctuations in a liquid induce to formation and collapse of bubbles, phenomenon known as cavitation (Fitch, 2002; Karimi and Martin, 1986). The repetitive impacts on a neighbor solid surface caused by the stress pulses generated from the bubbles implosion and microjets impingement are able to cause plastic deformation (Karimi and Martin, 1986; Santa et al., 2011), fatigue processes on the material surface (Richman, and Mcnaughton, 1990), and consequent mass loss by erosion. Such phenomenon can occur in almost all the hydrodynamic systems and turbomachines, as well as pumps, marine propellers, hydraulic turbines, and others (Karimi and Martin, 1986), causing alteration of the performance of the system (Franc and Michel, 2006), and high maintenance costs, since the cavitation erosion is the major failure mechanism of many fluid machinery components (Tzanakis et al., 2017). In view of the detrimental cavitation effects, several researches have been conducted in materials engineering field, aiming properties or characteristics, which can promote improved performances on cavitation erosion resistance.

According to Barlow and Du Toit (2012), medium-carbon AISI 420 MSS has high strength and excellent wear resistance in hardened and tempered condition, which makes it ideal for applications as cutlery, hand tools, dental and surgical instruments, valve trim and parts, shafts, and plastic molding. Moreover, regarding the MSS, a specific use of this steel grade is for the manufacture of power drive shafts in mildly aggressive environments, steam turbine blades or

compressor blades, and others (Boniardi and Casaroli, 2014). However, even the steel presenting high mechanical resistance and wear resistance (Boniardi and Casaroli, 2014), for applications that require better surface performance, such as in materials subjected to the cavitation phenomenon, the surface properties of MSSs should be increased. In this sense, plasma assisted thermochemical treatments are used, as successful techniques to improve cavitation erosion resistance of martensitic stainless steels (Allenstein et al, 2013; Allenstein et al, 2014; Espitia et al., 2013; Espitia et al., 2015; Pant et al., 2012). Nevertheless, up to the moment, only the use of nitriding (Allenstein et al, 2013; Allenstein et al, 2014; Espitia et al., 2013; Espitia et al., 2015), and nitrocarburizing (Pant et al., 2012) treatments have been reported in the literature, being the present study the first to use the plasma carburizing technique aiming to improve the MSS surface cavitation erosion resistance, at least in the authors knowledge. Thereby, this work intends to analyze the potential of plasma-assisted carburizing technique in improving the cavitation erosion resistance of martensitic stainless steels.

2. EXPERIMENTAL PROCEDURE

2.1 Material and treatments

2.1.1 Reference samples

As-received 50.8 mm diameter bar of AISI 420 MSS, in annealed condition, presenting a microstructure constituted by a ferritic matrix and esferoidized carbides was used as raw-material for the samples preparation. The chemical composition obtained by optical emission spectrometry was 0.305% C, 0.33% Si, 0.33% Mn, 0.019% P, 0.005% S, 12.21% Cr, 0.38% Ni, 0.025% Mo, 0.077% Cu, 0.006% Al, 0.043% V, 0.08% Nb, and Fe in balance, in wt.%. Samples of 10 mm thickness were cut and austenitized at 1050 °C during 0.5 h and air cooled, aiming to obtain a martensitic microstructure. Subsequent tempering was performed, in order to obtain the reference sample condition. In this case, as-quenched specimen was tempered at 220 °C for 1 h and air cooled to room temperature. The heat treatments were carried out in a vacuum furnace. The reference samples presenting microstructure constituted by the martensite, undissolved chromium carbide and cementite phases were aftermost ground using SiC sandpaper (up to 1200 grade) and mirror polished using 1 μm Al_2O_3 abrasive suspension.

2.1.2 Plasma carburizing treatment

Plasma carburizing treatment was performed in as-quenched samples, which provided a microstructure constituted by (untempered) martensitic matrix and undissolved chromium carbide precipitates. The samples were ground, polished and cleaned in ultrasonic bath for 10 min, dried in hot air flow, and then introduced into the discharge chamber. The carburizing thermochemical treatment was performed at 350 °C for 12 h, employing a gas mixture of 99.5% (80% H_2+20% Ar) + 0.5% CH_4, flow rate of 1.67×10^{-6} m^3s^{-1} and pressure of 400 Pa, after a previous cleaning step carried out in a hydrogen-argon glow discharge at 300 ºC temperature. A detailed description of the plasma apparatus and the electrical discharge parameters used in present work can be found in Scheuer et al. (2012; 2013).

2.2 Microstructure and hardness

The samples microstructure was analyzed by XRD technique using an XRD 7000 X-ray diffractometer with Cu Kα X-ray tube in the Bragg-Brentano θ-2θ configuration. The XRD patterns were obtained employing scanning interval (2θ angles) from 35 to 50 degrees and 0.05 degrees/min scanning speed. The hardness measurements were determined using an HMV-2T Shimadzu micro-hardness tester, applying a 300 gf load for the untreated samples and a 25 gf load for carburized samples, with peak-load contact of 15 s.

2.3 Cavitation erosion tests

Cavitation erosion tests were carried out in accordance with ASTM G32-10 standard. The vibratory ultrasonic equipment was set by the indirect method test configuration. The apparatus setup is schematically presented in Figure 1. Samples were cut by water jet technique in 33 x 20 x 10 mm^3 dimensions (proper to be attached to the sample support). Samples were placed to 500 μm distance of the vibratory horn tip. The test liquid was distilled water, which temperature was monitored by means of a thermocouple device and controlled by a cooling bath of a cooled and transient water flux, in order to limit the distilled water to the 25 ± 2 ºC temperature range. Vibration frequency was 20 KHz, the peak-to-peak displacement amplitude of the horn was 50 μm and the immersion deep of the sample tested (33 x 20 mm^2) surface in distilled water was 12 mm. The cumulative mass loss of the specimens was determined by means of 0.1 mg precision balance.

Mass loss versus testing time curve was determined from the average mass loss obtained for two different samples of each studied condition. Testing duration was 18 h for untreated samples and 28 h for carburized samples (tests were

performed till the maximum-erosion rate period was reached). Nominal incubation time was determined according ASTM G32-10 procedure, from the intercept of the straight-line extension of the cumulative mass loss-time curve's maximum-slope portion on the time axis. Finally, the cavitation-erosion surface damage for both the studied conditions was evaluated by means of scanning electron microscopy (SEM), using a TESCAN VEGA 3 LMU SEM.

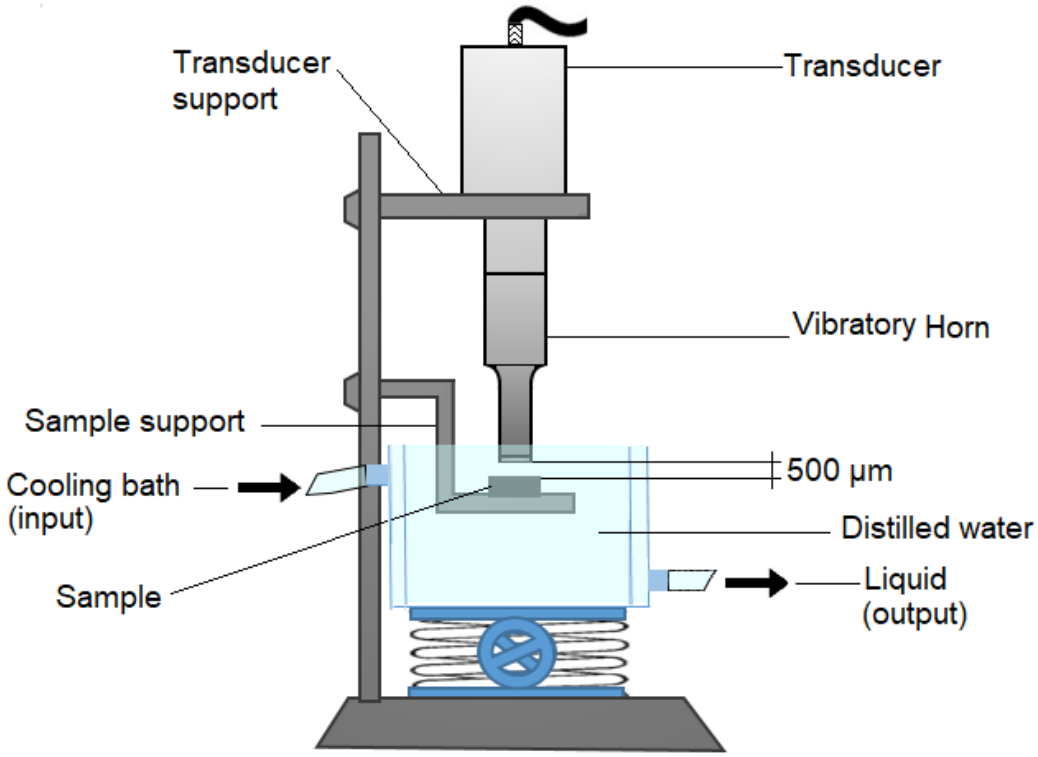

Figure 1. Cavitation test by indirect method

3. RESULTS AND DISCUSSION

3.1 X-ray diffraction analysis

Figure 2 shows the X-ray diffraction patterns of untreated and plasma carburized samples. Regarding to untreated samples, it can be seen an asymmetrical peak related to Fe_3C phase (43.92° degree), identified at the left-side of α' phase peak, which is a result of the tempering process of the reference sample, supposedly leading the martensite structure to be changed from b.c.t. to b.c.c.. Nevertheless, in spite of it, the X-ray diffraction pattern still presents the main peak at 44.8° degree, which is attributed to the martensite phase (α'), being in accordance with the expected for the low-temperature tempering and with the substantial carbon content of the studied steel.

In relation to the carburized samples, some significant changes can be observed after the carburizing treatment. First, the martensite peak was broadened and slightly shifted to lower angle (~ 44.32°), indicating (compressive) residual stress occurrence and lattice parameter expansion, respectively. Second, from the α'-peak position shift, it can be also expected that during the treatment, the carbon diffusion into the martensite phase tends to result in its carbon content enhancement, forming the so called carbon-expanded martensite phase (α'_C), as previously presented by Angelini et al. (2016) and Scheuer et al. (2012; 2013). Likewise, Fe_3C peaks are clearly distinguished at 39.78, 43.23 and 45.96° reflections.

3.2 Surface characteristics and hardness

The SEM images of AISI 420 plasma carburized at 350 ºC presented a rough surface aspect, which is characterized by the presence of island-like particles nucleated at the surface, as it can be seen in Figure 4a ahead. According to Chapman (1980), sputtered atoms from the cathode surface can backscatter in the plasma phase, moving back to the original surface and condensate on the substrate surface.

On the other hand, micro-hardness measurements show average values of 610 ± 15 $HV_{0.3}$, and 820 ± 40 $HV_{0.025}$ for untreated, and treated samples top surface, respectively, indicating a hardness increment in order of 1.3 times after carburizing treatment.

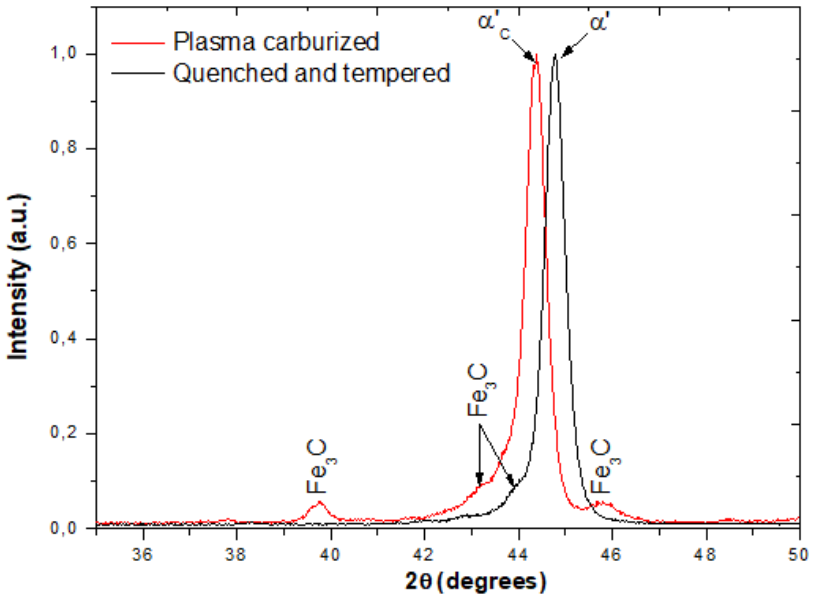

Figure 2. X-ray diffraction patterns of untreated (quenched and tempered) and plasma carburized AISI 420 MSS samples.

3.3 Cumulative mass loss

Figure 3 presents the cumulative mass loss (CML) as a function of the cavitation erosion testing time for the untreated (quenched and tempered) and plasma carburized samples. It was evidenced that the cavitation erosion resistance of the low-temperature plasma carburized AISI 420 martensitic stainless steel is strongly increased in relation to the untreated material (related to the quenched and tempered reference condition). From Figure 3 it is verified an incubation period around 6.3 h for the quenched and tempered reference condition samples, while the carburized samples show mass loss starting from 11.3 h testing time, which means that the AISI 420 MSS presented an increase of approximately 1.8 times in the cavitation erosion incubation period, after carburizing treatment application. In addition, nominal incubation periods of 7.8, and 17.9 h for the untreated, and carburized samples were observed, respectively. This result is due to the increased surface hardness, promoted by the carburized layer (α'_C + Fe_3C) formation, which leads to the obtainment of a more resilient surface. The cavitation performance of the carburized samples indicates the very well established correlation between hardness and cavitation erosion resistance for the material, corroborating with Hattori and Ishikura (2010), and Heathcoc et al. (1982) observations, concerning stainless steels.

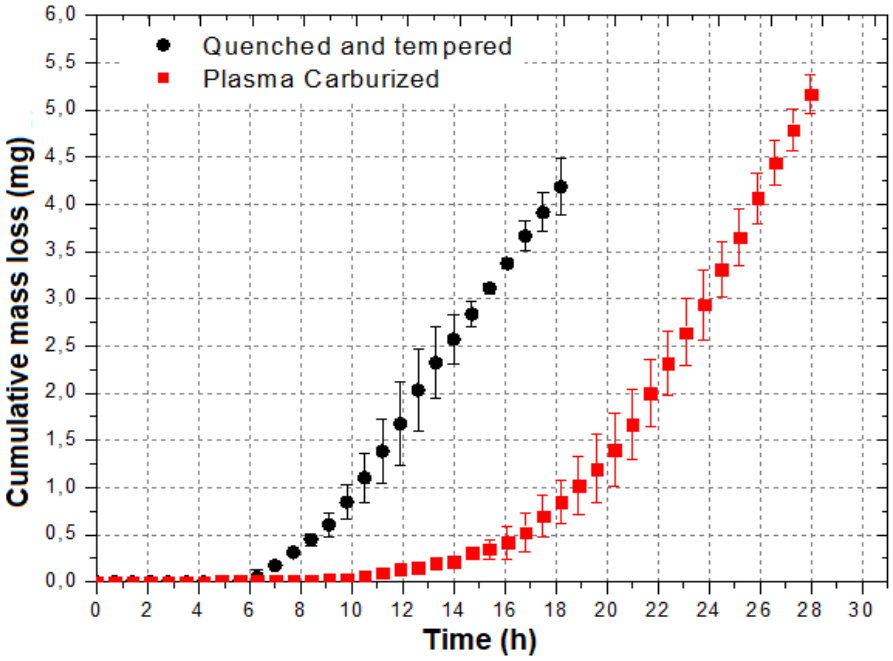

Figure 3. Cumulative mass loss (CML) as a function of the cavitation exposure time for untreated (quenched and tempered) and plasma carburized samples.

3.3 Surface damage

3.3.1 Untreated condition

Figure 4(a; b, b.1; c, c.1) shows the surface morphology aspect for untreated sample before the cavitation erosion testing; after 4 h cavitation testing time for two different magnitudes; and after 9 h cavitation testing time for two different magnitudes. Untreated sample presents an initial smooth aspect (Figure 4a), which is typical for polished surfaces. Pre-existent defects (pores) can be seen in the studied surface (indicated by arrows 1). After 4 h testing time (time interval that is inside the incubation period, which means none or negligible mass-loss), it is verified that the untreated sample (Figure 4b, b.1) presents evidences of plastic deformation, since small undulations (arrows 2) can be observed (probably embossing the original martensite laths). It is supposed that the parent austenite grain boundaries were also revealed (see arrow 3), as a result of material flow, similarly to reported by Espitia et al. (2015), however, the changes on the surface here observed are lesser pronounced than the presented by those authors, as a consequence of the too small ductility demonstrated for the present material, corroborating with its relatively high hardness. This surface aspect occurs because dislocations are created during plastic deformation and dislocation lines cannot begin or end within the crystal, thus new dislocations can be created either innerly to the crystal surfaces, especially at grain boundaries, or in special configurations (Rösler and Harders, 2007). During the incubation period, the non-treated material responds to cavitation by elastic and plastic deformation. After reached the material strength limit, the strain hardened regions become less resistant to stresses generated by cavitation and act as initiation sites of erosion (arrow 4), as shown in Figure 4(b, b.1). This statement is supported by surface morphology after 9 h testing time (Figures 4c, c.1), which appearance suggests the erosion taking place mainly from grain boundaries (arrows 6).

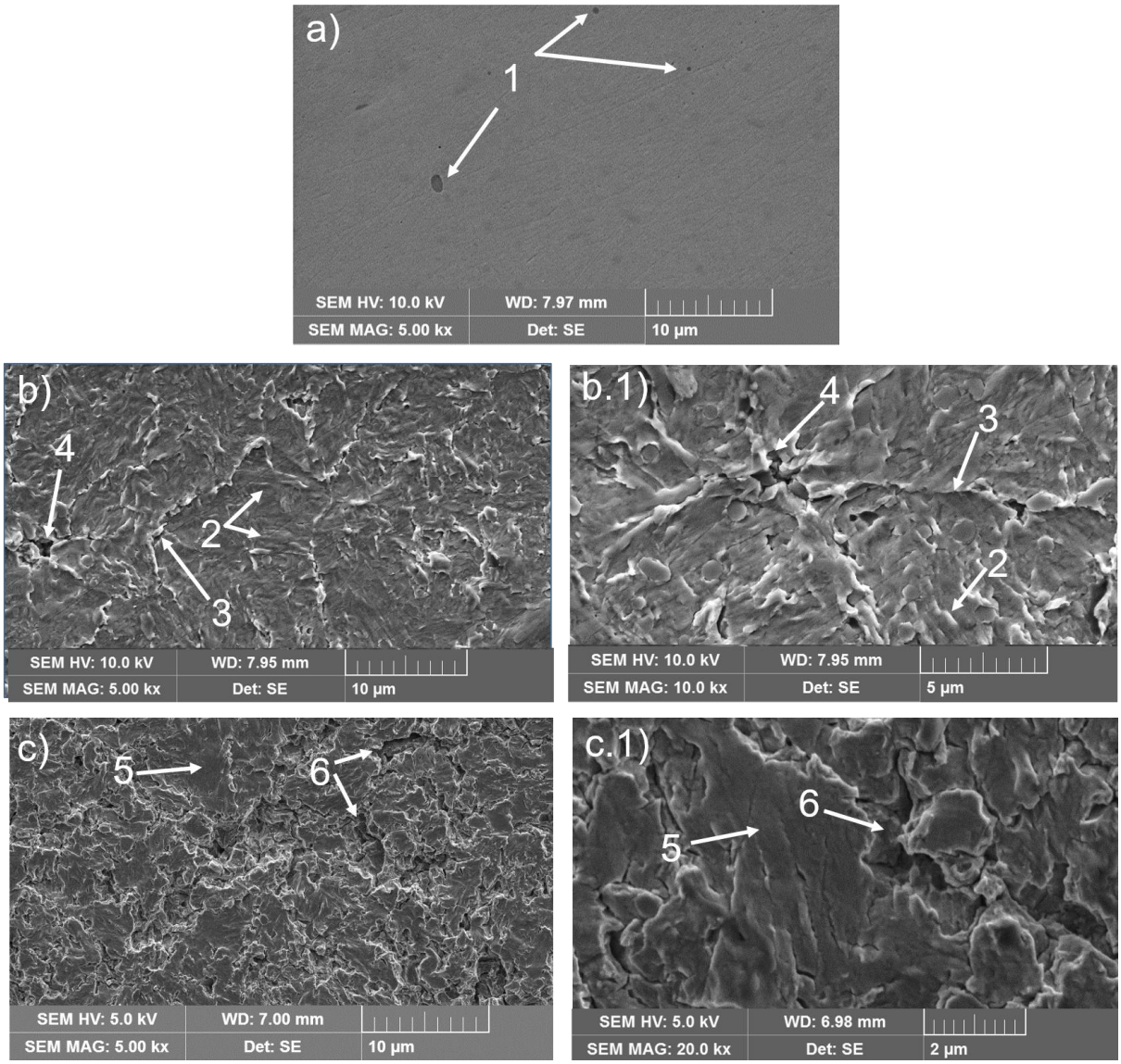

Figure 4. Surface morphology aspect for untreated sample: a) before cavitation erosion test; b) and b1) after 4 h cavitation testing for two different magnitudes; and c) and c1) after 9 h cavitation testing for two different magnitudes.

Figure 5 demonstrates the worn surface after 18 h testing time. Figure 5a.1 presents the detail in higher magnitude image from Figure 5a. In Figure 5a.1 it is possible to observe a deep hollow probably previously existent on the material surface before cavitation test (as shown in Figure 4a), that could have been enlarged by cavitation erosion, trough debris cracking in its boundaries. The arrows show that cracks also propagate inside the bulk direction.

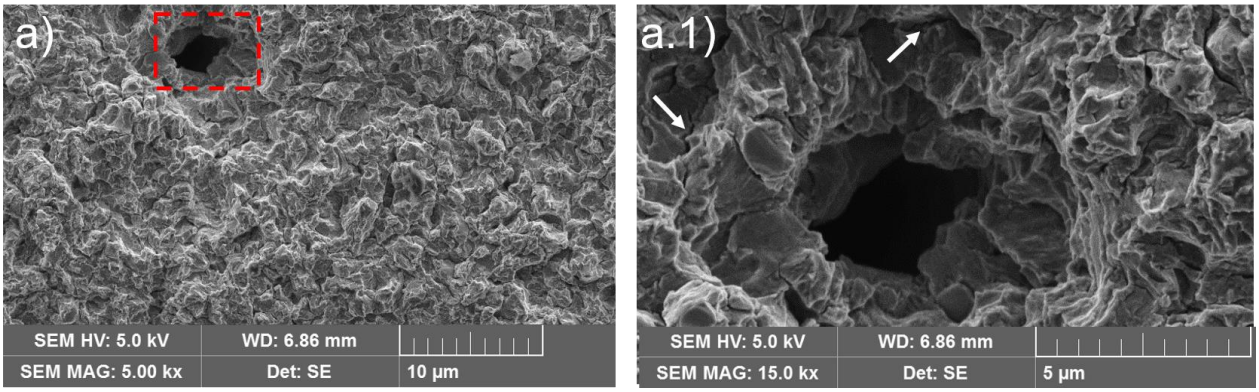

Figure 5. Worn surface for untreated sample after 18 h testing time.

3.3.2 Carburized sample

Figures 6 and 7 show the wear evolution on the carburized sample surface. Cavitation exposure tends to remove the like-island particles (arrow 1), previously observed to cavitation testing from the surface (Figure 6a). At 1.3 h testing, some residuals particles can be seen (Figure 6b), in addition, some superficial pores (as presented by untreated condition previously to cavitation erosion testing, in Figure 4a) before occult by those particles can be seen. After 4 h testing (Figure 7a), the island-like particles have been totally removed and then the sample presents a surface nearest to smooth aspect. At this time, cavities (arrow 1) and thin shallow cracks connected (arrows 2) or around it (arrow 3) appear. Figure 7a.1 shows in higher magnitude that initial cracks arise from surface defects borders (arrow 2), as well as the first debris formation appears, still in the incubation period. Finally, after 13 h testing (time which the incubation period was exceeded, as shown in Figure 7b, it is possible to verify deeper cracks (arrow 4) on the surface, which ones convert in craters and expand by formation (arrow 5) and detaching of debris. It is to be observed the absence of plastic deformation on the cavitation erosion tested surface, which characterizes the elastic response of the carburized surface when subjected to cavitation generated stresses during the incubation period, being the carbon-rich layer eventually removed by a brittle manner (arising and deepening of cracks and posterior cracks broadening into craters). On the other hand, the increased incubation period presented for this condition suggests the increment in the elastic deformation capacity of the treated surface, which characterizes a more resilient surface.

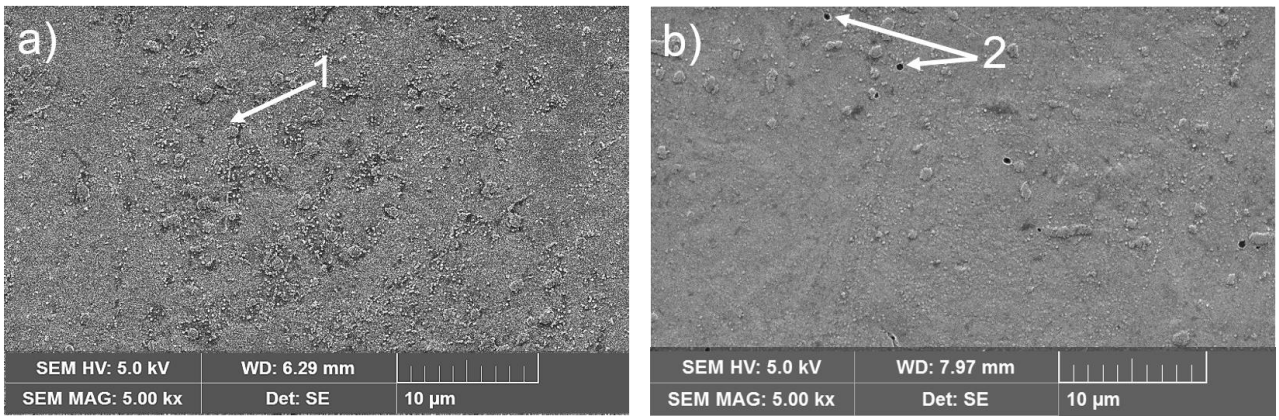

Figure 6. Removal of island-like particles during initial moments of cavitation testing.

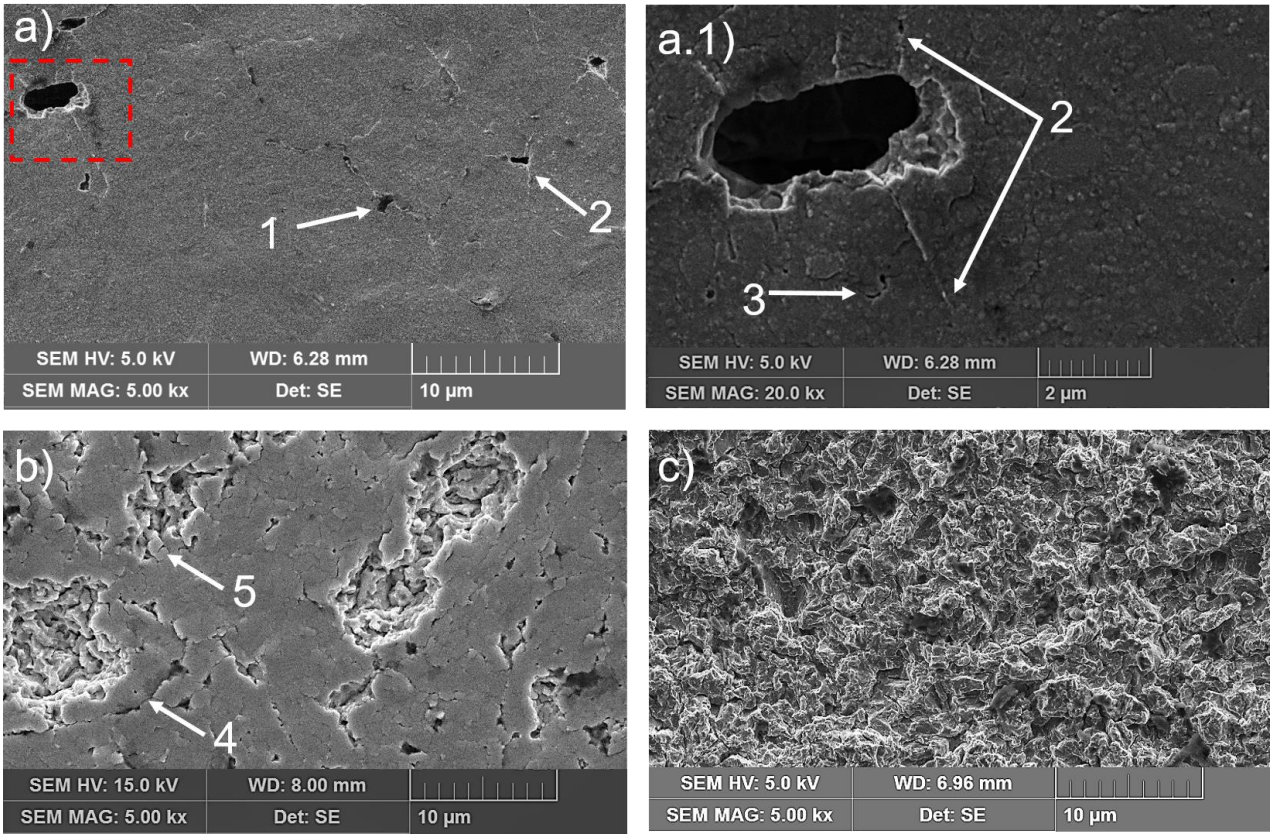

Figure 7. Evolution of the damage on the surface for carburized condition: a) and a1) after 4 h testing; b) after 13 h testing and c) after 28 h testing.

4. CONCLUSIONS

By the results, it can be concluded that low-temperature plasma carburizing can be successfully employed to increase the AISI 420 martensitic stainless steel cavitation erosion resistance. The incubation time for cavitation erosion of plasma carburized sample increases around 1.8 times compared to untreated samples, and such increment in cavitation erosion resistance after carburizing treatment follows the surface hardness increment. The quenched and tempered sample presented some plastic deformation during incubation period whereas carburized samples showed no plastic deformation evidence. Both conditions presented debris fracture as the main wear mechanism. This first investigation showed promising results concerning MSS cavitation erosion resistance by means of low-temperature plasma carburizing treatment.

5. ACKNOWLEDGMENTS

The authors acknowledge the support of CNPq, CNPq-Universal Grant N. 482380/2012-8, and the MCTI/CNPq/CT-Aquaviário Grant N. 456347/2013-5, and state the sincere thanks to the Laboratory of X-ray Optics and Instrumentation (LORXI-UFPR) for the use of XRD equipment, the Electronic Microscopy Center (CME-UFPR) for the use of the equipments, and to Mr. Flavio Stramare Ribeiro and AQUACORT company for the assistance in cutting the samples.

6. REFERENCES

Allenstein, A.N.; Lepienski, C.M.; Buschinelli, A.J.A.; Brunatto, S.F. Plasma nitriding using high H2 content gas mixtures for a cavitation erosion resistant steel. Applied Surface Science 277 (2013) 15–24.

Allenstein, A.N.; Lepienski, C.M.; Buschinelli, A.J.A.; Brunatto, S.F. Improvement of the cavitation erosion resistance for low-temperature plasma nitrided Ca-6NM martensitic stainless steel. Wear 309 (2014) 159–165.

ANGELINI, V. et al. Dry sliding behavior (block-on-ring tests) of AISI 420 martensitic stainless steel, surface hardened by low temperature plasma-assisted carburizing. Tribology International, v. 103, p. 555-565, 2016.

BARLOW, Lilian D.; DU TOIT, Madeleine. Effect of austenitizing heat treatment on the microstructure and hardness of martensitic stainless steel AISI 420. Journal of materials engineering and performance, v. 21, n. 7, p. 1327-1336, 2012.

Boniardi, Marco; Casaroli, Andrea. Stainless Steels. Lucefin, 2014.

Espitia, L.A.; Varela, L.; Pinedo, C.E.; Tschiptschin, A.P. Cavitation erosion resistance of low temperature plasma nitrided martensitic stainless steel. Wear 301 (2013) 449–456.

Espitia, L. A. et al. Cavitation erosion resistance and wear mechanisms of active screen low temperature plasma nitrided AISI 410 martensitic stainless steel. Wear, v. 332, p. 1070-1079, 2015.

Fitch, E. C. Cavitation wear in hydraulic systems. Machinery Lubrication Sept, 2002.

Franc, Jean-Pierre; Michel, Jean-Marie. Fundamentals of cavitation. Springer Science & Business Media, 2006.

Hattori, Shuji; Ishikura, Ryohei. Revision of cavitation erosion database and analysis of stainless steel data. Wear, v. 268, n. 1, p. 109-116, 2010.

Heathcock, C. J.; Protheroe, B. E.; Ball, A. Cavitation erosion of stainless steels. Wear, v. 81, n. 2, p. 311-327, 1982.

Karimi, A.; Martin, J. L. Cavitation erosion of materials. International Metals Reviews, 1986.

Pant, B.K.; Arya, V.; Mann, B.S. Cavitation Erosion Characteristics of Nitrocarburized and HPDL-Treated Martensitic Stainless Steels. Journal of materials engineering and performance 21 (2012) 1051–1055.

Richman, R. H.; Mcnaughton, W. P. Correlation of cavitation erosion behavior with mechanical properties of metals. Wear, v. 140, n. 1, p. 63-82, 1990.

RÖSLER, Joachim; HARDERS, Harald; BAEKER, Martin. Mechanical behaviour of engineering materials: metals, ceramics, polymers, and composites. Springer Science & Business Media, 2007.

Santa, J. F. et al. Cavitation erosion of martensitic and austenitic stainless steel welded coatings. Wear, v. 271, n. 9, p. 1445-1453, 2011.

Scheuer, C.J.; Cardoso, R.P.; Pereira,l R.; Mafra M.; Brunatto, S.F. Low temperature plasma carburizing of martensitic stainless steel. Materials Science and Engineering A, v. 539, p. 369-372, 2012.

Scheuer, C. J. et al. AISI 420 martensitic stainless steel low-temperature plasma assisted carburizing kinetics. Surface and Coatings Technology, v. 214, p. 30-37, 2013.

Tzanakis, I. et al. Evaluation of Cavitation Erosion Behavior of Commercial Steel Grades Used in the Design of Fluid Machinery. Metallurgical and Materials Transactions A, v. 48, n. 5, p. 2193-2206, 2017.

7. RESPONSIBILITY NOTICE

The authors are the only responsible for the printed material included in this paper.